

Lower Ordovician reversal asymmetry: An artifact of remagnetization or nondipole field disturbance?

Trond H. Torsvik

Geological Survey of Norway, Trondheim

Allan Trench

Western Mining Corporation, Kambalda, Western Australia

Kyger C. Lohmann and Shannon Dunn

Department of Geological Sciences, University of Michigan, Ann Arbor

Abstract. Five stratigraphically linked polarity intervals (R1→R5 and N1→N5) from Late Arenig to Early Caradoc (Ordovician) times are recognized within the Gullhøgen Limestone section, southern Sweden. The reversal frequency should be considered as a minimum given extremely low sedimentation rates (1–3 m/m. y.). Primary magnetite, probably detrital or biogenic in origin, is the prevailing remanence carrier in addition to early diagenetic hematite. A conspicuous reversal asymmetry, in which the remanence directions of the two lowermost normal polarity sections (N1 and N2) depart significantly from otherwise nearly antiparallel and typical Lower Ordovician directions, has been identified. This reversal asymmetry is mainly in declination. An artifact of remagnetization cannot be entirely ruled out, but we find this explanation rather unsatisfactory given the lack of systematic magneto-mineralogical or isotope variations ($\delta^{18}\text{O}$ and $\delta^{13}\text{C}$) within these anomalous normal polarity horizons. The anomalous strata involved do not exhibit a different degree or extent of diagenetic alteration or magnetomineralogical character when compared to horizons above and below carrying the reverse polarity directions. We therefore suggest nonzonal nondipole field disturbances, lasting some 1–1.5 m. y. as a likely source, in order to explain these normal polarity anomalies. If the observations appear to be global, the results question the fundamental palaeomagnetic concept of symmetric reversals throughout geological time.

Introduction

In 1978, Claesson published the first palaeomagnetic data from autochthonous or parautochthonous Ordovician successions outcropping in several districts in southern Sweden [Thorslund and Jaanusson, 1960; Thorslund, 1962; Lindström, 1971]. Claesson [1978], however, questioned the reliability of her own data and considered the data to be unrepresentative of the Ordovician paleofield. The paleomagnetic data were therefore depicted as anomalous in the literature for more than a decade.

In a reexamination of the original data sets of Claesson [1977], Torsvik and Trench [1991a] revised the original interpretation and pointed out the presence of polarity reversals and statistically positive fold tests in the original data sets. A stratigraphically linked reversal pattern, of Llanvirn–Caradoc age, was subsequently established by Torsvik and Trench [1991b] for the Swedish sections whilst a global correlation of Ordovician data was attempted by Trench *et al.* [1991].

Early Ordovician times (Tremadoc–Arenig) were dominated by a reverse polarity field, whilst rapid reversals occurred during

the Llanvirn and Llandeilo, and the Upper Ordovician shows a normal polarity field bias [Trench *et al.*, 1991]. In this account we report new Late Arenig to Early Llanvirn paleomagnetic and stable isotope data from Vestergötland (Gullhøgen Quarry), southern Sweden (Figure 1). We have identified several polarity reversals during this time interval, hitherto not recognized in the Swedish sections, but with a conspicuous long-lasting (m. y. scale) reversal asymmetry which, if global, may shed doubts on the basic assumption that the mean geomagnetic field equates to a geocentric axial dipole field throughout Phanerozoic times. Suggestions of Middle Proterozoic asymmetric field behavior have previously been uncovered by for example Pesonen and Nevalinna [1981].

Geology and Sampling

The Gullhøgen Quarry, southern Sweden (Figure 1), contains approximately 70 m of Upper Cambrian to Upper Ordovician strata [Thorslund and Jaanusson, 1960; Jaanusson, 1964; Jaanusson, 1982; Holmer, 1989]. Remarkably slow sedimentation rates (1–3 m/m. y.) are indicated, but significant disconformities have been observed in the section. It is disputed, however, whether these intervals of nondeposition formed as submarine hardgrounds or represent periodic emergence [Lindström, 1971; Jaanusson, 1982; Holmer, 1983]. The section



Figure 1. Geographic location of the study area (Gullhøgen Quarry) in southern Sweden.

is flatlying, undeformed, and capped by Permo-Carboniferous dolerite sills (287 ± 14 Ma; K/Ar [Mulder, 1971]). These sills served as an erosional protection for the Cambro-Ordovician successions, but they caused considerable thermal (TRM) and/or thermo-chemical (TCRM) overprinting, with the upper part of the section (Middle-Caradoc) being entirely dominated by Permo-Carboniferous (P-C) magnetic overprints [Torsvik and Trench, 1991b].

The upper part of the section (Middle-Llanvirn to Caradoc) has been described in detail by Holmer [1989], and the palaeomagnetic signature of these intervals has been studied by Torsvik and Trench [1991b]. In decreasing stratigraphic order (Figure 2) this section embraces the Dalby Limestone (gray carbonate mudstones and nodular calcarenites), the Ryd Limestone (mainly gray carbonate mudstone), the Gullhøgen Limestone (red, gray or variegated red-gray calcareous mudstone to fine nodular limestone), the Skövde beds (15-cm-thick variegated red and gray limestone), and the Vamb Limestone (limestone with red iron rich ooids and stromatolite structures). The Vamb Limestone, 12 cm in stratigraphic thickness, is bounded by discontinuity surfaces considered to delineate significant time gaps [Holmer, 1989].

The present study examines the Holen and Lanna Limestones (Late Arenig-early Llanvirn) and a few subordinate samples from the overlying Vamb Limestone and the Skövde Beds. New data on the stable isotope composition of these limestones is compared with paleomagnetic data derived from this and previous investigations (top 35 cm of Holen Limestone, Vamb Limestone, and Skövde Beds earlier studied paleomagnetically by Torsvik and Trench [1991b]).

The Holen Limestone forms part of a widespread lithofacies and biofacies, most commonly referred to as the Orthoceras Limestone. The Holen Limestone embraces red bedded calcilute in addition to thinner beds of red argillaceous calcilute, nodular red calcilute, and alternating layers of gray and pale red calcilute. It overlies the Lanna Limestone which is dominated by gray and light gray limestones. Eighty-one stratigraphic levels, with at least two drill cores at each level, were sampled with a portable drill. The total vertical section approximates 15 m (Figure 3),

but minor gaps are inevitable because of sampling inaccessibility of the quarry faces.

Natural Remanent Magnetization and Susceptibility

The natural remanent magnetization (NRM) was measured with either a three-axis superconducting magnetometer (2G) or an automatic spinner magnetometer (JR5A). The bulk susceptibility was measured with a Minisep bulk susceptibility head.

When considering the entire Gullhøgen section (Figure 2) [Torsvik and Trench, 1991b; this study], it is evident that variations in NRM intensity and bulk susceptibility closely relate to the coloring of the strata. Gray samples have lower values than those recorded in variegated red and gray samples, which in turn are lower than red colored samples. The NRM intensity, most notably in the uppermost strata, is affected by Permo-Carboniferous overprinting, and NRM intensities up to 500 mA/m in the uppermost level of the section are clearly attributable to this effect (Figure 2).

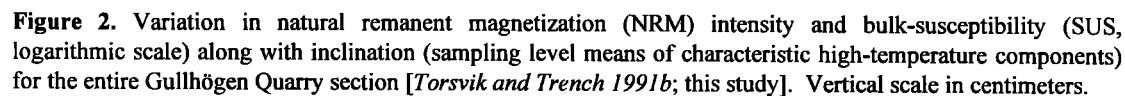
NRM intensity and bulk susceptibility for the Holen Limestone, mostly red, bedded calcilute, average to approximately 30 mA/m and 100×10^{-6} SI units, respectively (Figures 2 and 3). Maxima, up to 110 mA/m and 1700×10^{-6} SI units, but also large fluctuations (millimeter to centimeter scale) are observed in the uppermost part of the Holen Limestone and the overlying Vamb and Skövde Beds. There is a notable decrease in NRM intensity and bulk susceptibility down-section and local lows and highs usually correlate with the color of the strata, that is, minima are usually associated with gray limestone beds.

The Lanna Limestone, mostly gray and light gray limestones, shows on average lower NRM intensities and bulk susceptibilities than the Holen Limestone. Local maxima are associated with dark gray, reddish colored, or thin zones of mottled red/gray limestone (Figure 3). In the lowermost part of the Lanna Limestone (light gray limestone) NRM intensity and bulk susceptibility decrease to approximately 3 mA/m and 40×10^{-6} SI units, respectively (Figure 3).

Thermomagnetic Analysis and Isothermal Remanent Magnetization Curves

Torsvik and Trench [1991b] concluded that magnetite was the prevailing opaque phase in the gray colored limestones of the Gullhøgen section (e.g., the Dalby Limestone; Figure 2). Isothermal remanent magnetization (IRM) curves for the Lanna Limestone (gray limestone) are dominated by a low-coercivity phase which is saturated in fields of 250–300 mT (Figure 4). This, along with Curie temperatures at around 570°C and the thermal unblocking spectra suggests magnetite as the principal remanence carrier in the Lanna Limestone. Samples from the lowermost stratigraphic levels of the Lanna Limestone, however, display large mineralogical changes during heating as evidenced from large increases in saturation magnetization after cooling (Figures 5a and 5b). The cooling curves indicate production of a secondary phase with Curie temperatures of 580°–600°. This phase, however, is metastable, and recycling of the daughter product suggests that the secondary magnetite oxidizes to a stable hematite phase during thermal recycling.

The Holen Limestone is often dominated by two phases; one subordinate low-coercivity phase (Figure 4) with Curie



reduction of hematite to magnetite. Samples from the Hølen limestone do not show saturation in the maximum available field (1200 mT in Figure 4). IRM intensities at this peak field vary between 3 and 7 A/m, an order of magnitude above the IRM saturation intensity recorded for the Lanna Limestone (typically around 0.1 A/m).

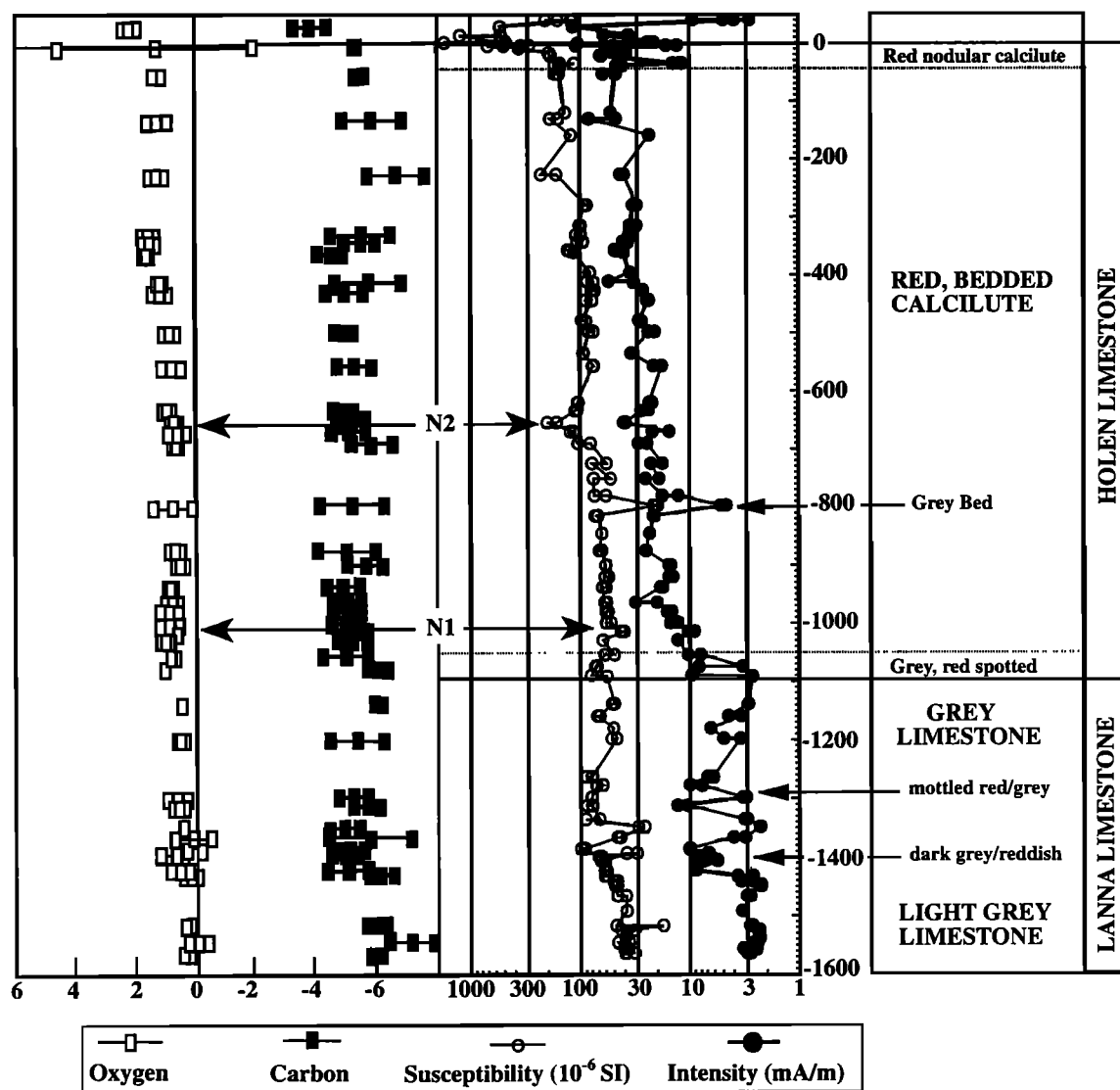


Figure 3. Variation in $\delta^{18}\text{O}$ and $\delta^{13}\text{C}$ (data represent mean values and confidence intervals for each stratigraphic horizon) along with natural remanent magnetization (NRM) intensity (mA/m) and bulk-susceptibility (10^{-6} SI) for the Hølen and Lanna Limestones (logarithmic scale). Vertical scale in centimeters.

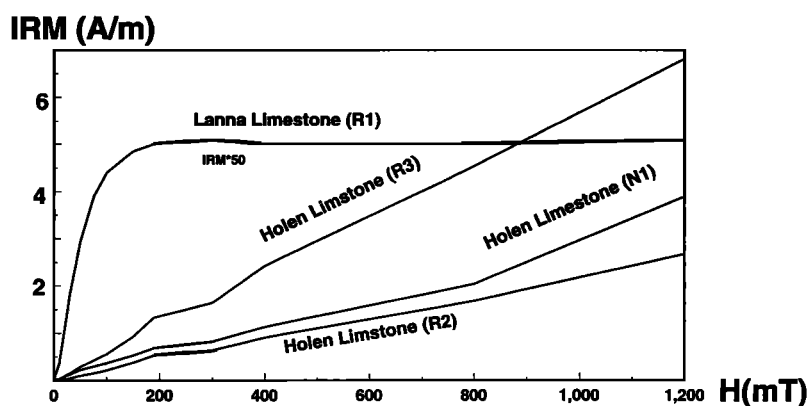


Figure 4. Isothermal remanence magnetization (IRM) acquisition curves for samples from the Lanna and Hølen Limestones. Note that IRM values for the Lanna Limestone is expanded 50 times.

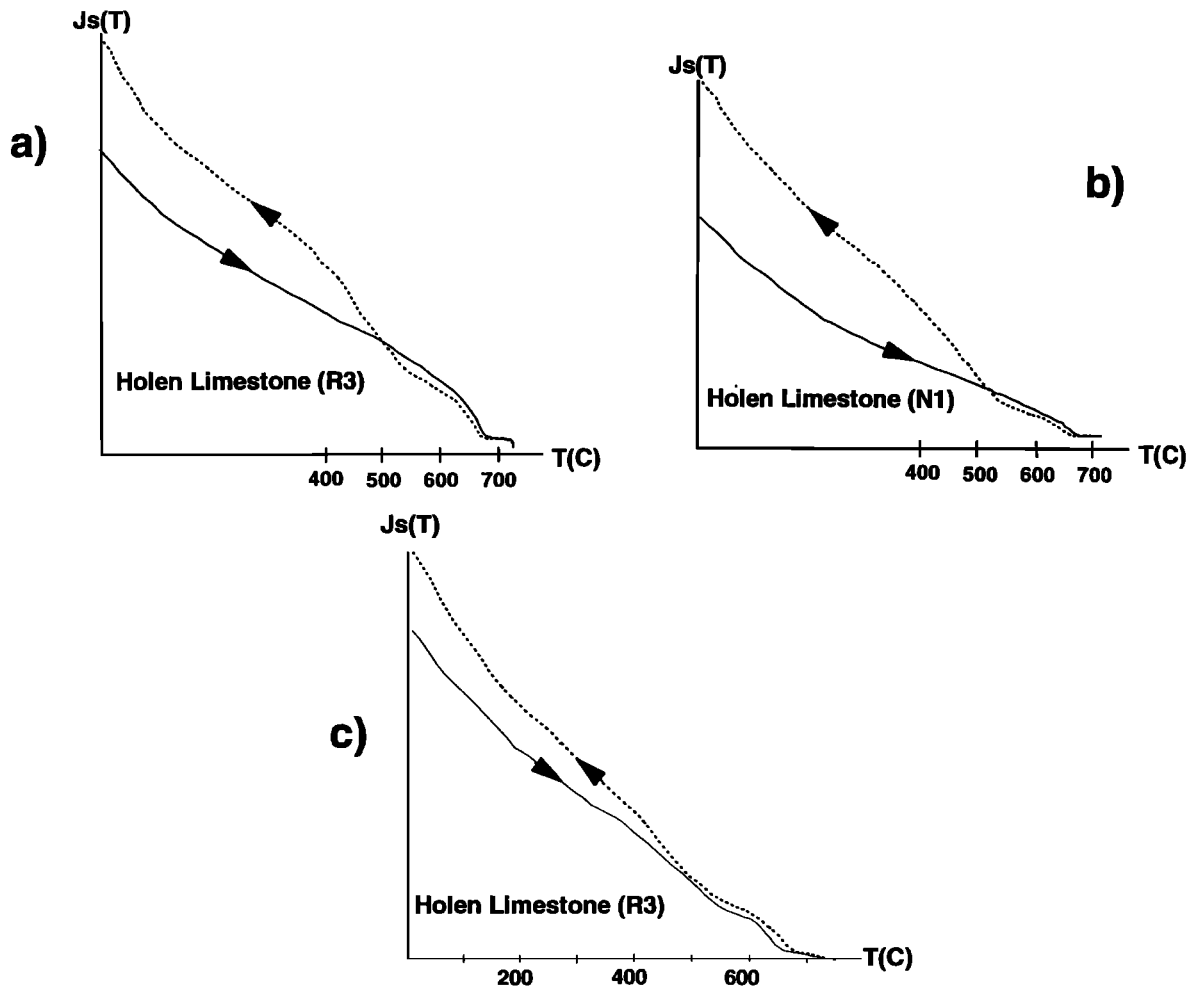


Figure 5. Thermomagnetic curve from the Lanna Limestone.

Directional Data: Lanna Limestone

The stability of NRM for a total of 179 samples was tested by means of stepwise thermal demagnetization. Characteristic remanence components were calculated using least squares analysis.

All the samples of predominantly gray limestones are dominated by a shallow component with negative inclinations

and SSW declinations (Figure 7a). This component, a Permo-Carboniferous (P-C) overprint [see *Torsvik and Trench, 1991b*] is comparable with palaeomagnetic data from the overlying sill [Mulder, 1971] which has been dated to 287 ± 14 Ma (K/Ar). The P-C component is typically demagnetized between 200° - 500° C after removal of a low-unblocking viscous component. The high-unblocking components are characterized by southeasterly to easterly declinations and downward inclinations (Figure 7b),

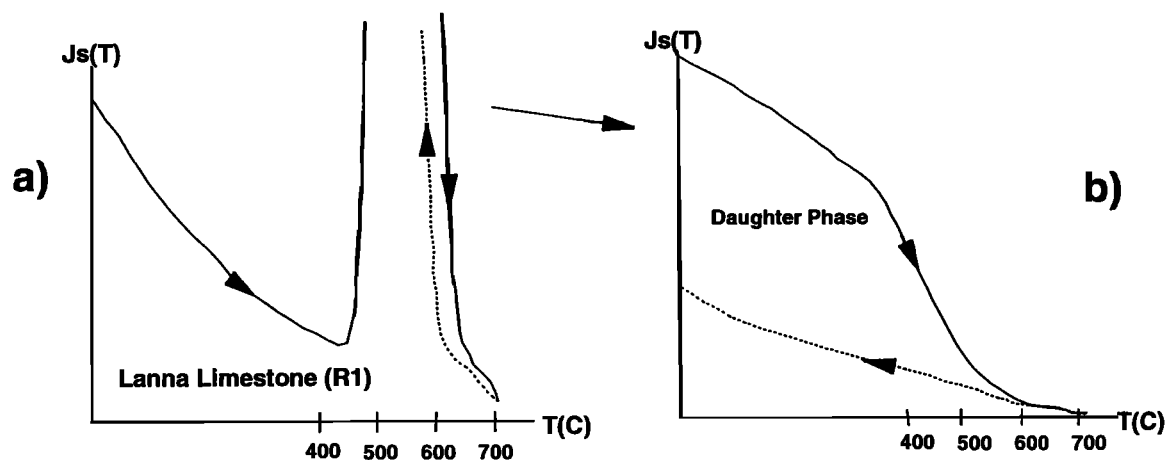


Figure 6. Thermomagnetic curves from the Holen Limestone.

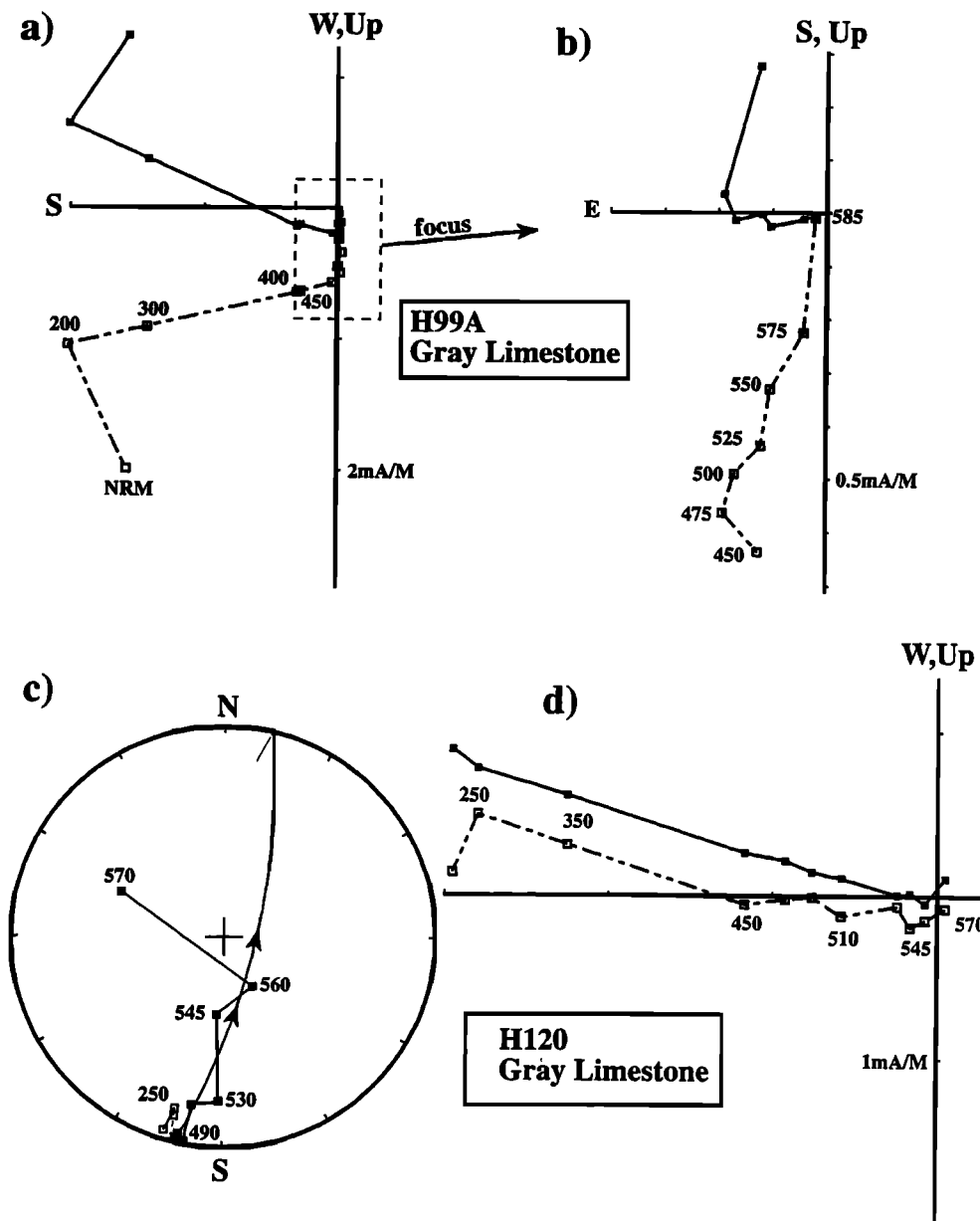


Figure 7. Examples of thermal demagnetization behavior for the Lanna Limestone (polarity zone R1). In orthogonal vector plots, points in the horizontal (vertical) plane are plotted as solid (open) symbols. In stereoplots, solid (open) symbols denote positive (negative) inclinations.

and comparable with Lower-Middle Ordovician aged directions reported from the higher stratigraphic strata [Torsvik and Trench, 1991b] or elsewhere in southern Sweden [Claesson, 1978; Torsvik and Trench, 1991a; Perroud et al., 1992]. In many cases, however, the P-C overprint component may almost obliterate the original Ordovician magnetic signature (Figures 7c and 7d). In the latter case, they all show a distinct great-circle trend toward the Ordovician field direction (reverse polarity) but failed to identify a stable end-point direction.

Altogether, 31 samples provided well-defined high-unblocking components with a directional grouping which is distinctly separated from the group of P-C overprint directions (Figure 8a). The high-unblocking components of the Lanna Limestone, all of reverse polarity (denoted R1), apparently have a magnetite host ($T_{b,max}=585^{\circ}\text{C}$).

Directional Data: Holen Limestone

The overlying Holen limestone, mainly red calcilute, contains several polarity transitions. The lowermost part is characterized by a normal polarity zone (N1), but we note that the high-unblocking normal polarity directions (Figure 8; Table 1) are not antipodal to the reverse polarity directions above and below N1. Most samples from normal polarity zones N1 and N2 appear to have a hematite host ($T_b=550^{\circ}\text{--}680^{\circ}\text{C}$) after having demagnetized the P-C component at temperatures below $450^{\circ}\text{--}500^{\circ}\text{C}$ (Figures 9a and 9b). Some samples, however, indicate a pure magnetite host (Figure 9c). Magnetite and hematite components, however, are directionally comparable, suggesting that remanence acquisition times are broadly comparable (from N1 to R2).

Exemplary thermal unblocking separation (discreteness) of the

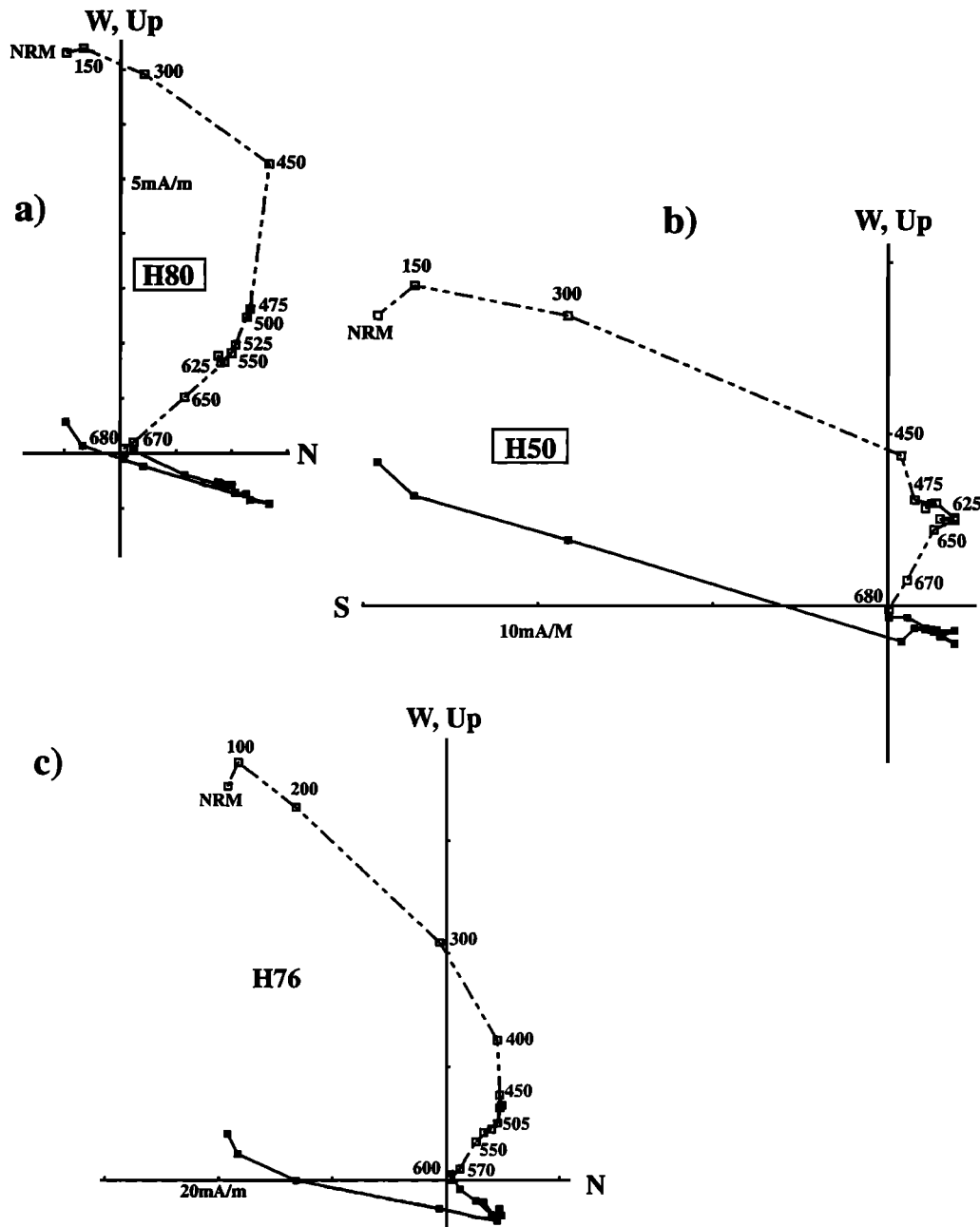


Figure 8. Distribution of characteristic remanence components from the Lanna (R1) and Holen Limestones (R2-R3 and N1-N2).

Ordovician and Permo-Carboniferous components is occasionally observed, most notably when the high-unblocking component appears to be carried by magnetite (R2, Figure 10a). Reverse polarity zone R2 is almost entirely dominated by magnetite as judged from the thermal unblocking spectra. Within polarity zone R3 we notice substantial blocking temperature overlap with the P-C component (Figure 10b, note the curved segment from 475°-650°C). In many cases the P-C component may have unblocking components that exceed that of the primary Ordovician paleofield direction. This is depicted in Figures 11a and 11b. The P-C component is identified in the 250°-450°C range, a reverse polarity Ordovician component is defined between 500° and 550°C (magnetite host?), and finally the shallow P-C component is once again indicated above 575°C

(hematite host). In many cases it is difficult to identify this high-unblocking component due to viscous directional behavior or component overlap. The example of Figures 11a and 11b indicates that some hematite has a secondary, Permo-Carboniferous origin, perhaps recording oxidation of primary magnetite. Consequently, the P-C components partly appear to have a chemical origin.

The quality of the normal polarity components is generally very good (Figure 9) except the uppermost sampling level of the N1 polarity zone which is clearly contaminated by reverse polarity directions (Figure 11c) in the intermediate-unblocking (525°-600°C) range. This probably reflects that the actual sample embraces the actual polarity transition.

Table 1. Paleomagnetic Data From the Gullhögen Quarry (Late Arenig-Early Llanvirn)

PZ	DEC,deg	INC,deg	N	α_{95}	k	Latitude	Longitude	δ_p/δ_m
R1	120.0	+61.4	31	8.0	11.5			
P-C	198.2	-13.8	34	2.4	103.0			
N1	023.2	-38.6	12	6.4	47.5			
P-C	201.6	-35.4	7	10.9	31.6			
R2	144.8	+52.5	8	10.4	29.4			
P-C	194.4	-14.6	16	4.5	67.5			
N2	015.1	-57.5	2	28.9	76.9			
P-C	197.9	-28.0	2	35.8	50.8			
R3	156.1	+48.6	25	7.5	15.9			
P-C	199.7	-13.3	42	3.1	50.7			
R1+2	126.3	+59.9	39	6.8	12.3	N18.7	E054.0	7.8/10.3
(R1+2+3	140.1	+56.4	64	5.5	11.4)			
N1+2	022.4	-41.3	14	6.5	37.8	S 5.9	E353.4	4.8/ 7.9
P-C	198.4	-15.4	101	2.1	47.2	S37.6	E350.7	1.1/ 2.2
R3*	140	+55	4	17.3	29.2			
N3	324	-41	1					
R4	134	+55	29	7.1	15.2			
N4	326	-66	6	6.6	104.2			
R5	127	+60	15	7.7	25.9			
Mean	134	+58	55	4.4	19.6	N14	E049	5.0/ 6.0
N5	335	-54	24	4.8	39.6	N 5	E034	5.0/ 7.0
P-C	198	-10	123	2.0	41.9	S35	E351	1.0/ 2.0

Geographic sampling coordinates, 58°3N and 13.9°E. *Palaeomagnetic data after *Torsvik and Trench* [1991b]. Note that they originally used polarity zones R1-R3 (now R3-R5) and N1-N2 (now N3-N5). R3 corresponds to the upper part of R3 listed above. PZ,= Polarity Zone; P-C,= Permo-Carboniferous overprint; DEC,INC,= mean declination /inclination; N,= number of samples; α_{95} ,= 95% confidence circle; k,= precision parameter [Fisher, 1953]; latitude/longitude,= paleomagnetic pole latitude/longitude; δ_p/δ_m ,= semi-axes of the cone of 95% confidence about the pole.

Variations in Carbon and Oxygen Isotopic Compositions

To evaluate the possibility that variations in the magnetic behavior of samples might reflect localized effects of diagenetic alteration, the $\delta^{13}\text{C}$ and $\delta^{18}\text{O}$ of the rock carbonate was determined from sampling of primary shell material, calcite cements and bulk analysis of the micritic carbonate matrix. Sampling was performed using a 500 μm dental bur which provides powdered carbonate of approximately 0.2 mg in weight. To obtain representative values for the bulk rock composition, three to eight sampling points were chosen from each rock specimen. Following sampling, all powders were roasted at 380°C in vacuo to remove volatile organic contaminants. Isotopic analysis was then performed on a Finnigan MAT 251 utilizing an on-line automated reaction system (Kiel Carbonate Device) which provides for reaction of samples in individual vessels to eliminate cross-sample contamination. Isotopic enrichments, reported relative to Pee Dee belemnite standard, were corrected for ^{17}O contribution following the procedures of *Craig* [1957]. Analytical precision was monitored through daily analysis of National Bureau of Standards powdered carbonate standards and was maintained better than 0.1‰ for both carbon and oxygen.

Mean compositional values and their confidence intervals are plotted for $\delta^{13}\text{C}$ and $\delta^{18}\text{O}$ in Figure 3. Carbon exhibits a monotonic increase in $\delta^{13}\text{C}$ from 0.0 to 1.5‰ over the length of the stratigraphic section. Such a range is compatible with estimates of primary marine $\delta^{13}\text{C}$ derived from previous studies [Veizer et al., 1980; Lohmann and Walker, 1989] and would

likely be modified only under extreme conditions of diagenesis involving high water/rock ratios. Only samples from the uppermost Holen Limestone, the Vamb Limestone (12 cm thick) and the Skövde beds (15 cm thick) deviate significantly from the typical trend. The Vamb Limestone, however, is bounded by upper and lower discontinuity surfaces [Holmer, 1983; 1989] which are associated with phosphatization and bleaching at and below the discontinuity surfaces. These discontinuity surfaces are characteristically marked by millimeter-scale drusy calcite indicative of more severe diagenetic alteration at these surfaces.

In contrast to carbon, the oxygen isotopic composition of carbonate is more readily altered in response to diagenetic alteration due to the isotopic exchange concomitant with fluid driven dissolution and precipitation reactions. Overall, $\delta^{18}\text{O}$ composition of our carbonate samples averages -5.0‰ (± 1.0 ‰). This average value is similar to estimated primary marine values derived from bulk micrite and abiotic marine cements. Significant deviations are observed only in the lowermost samples of the Lanna Limestone where values are slightly more negative, and in the uppermost Holen Limestone, the Vamb Limestone and the Skövde beds, where the values become less negative and more variable. In the latter cases, changes are easily attributable to increased diagenetic alteration below discontinuity surfaces. We notice that the variability in $\delta^{18}\text{O}$ composition in the uppermost section corresponds to large short-waved fluctuations (millimeter-centimeter scale) in bulk susceptibility and NRM intensity (Figure 3).

At several intervals, rock cores were more extensively sampled (six to eight analyses per core) to ensure that the full range of compositional variation was determined. These

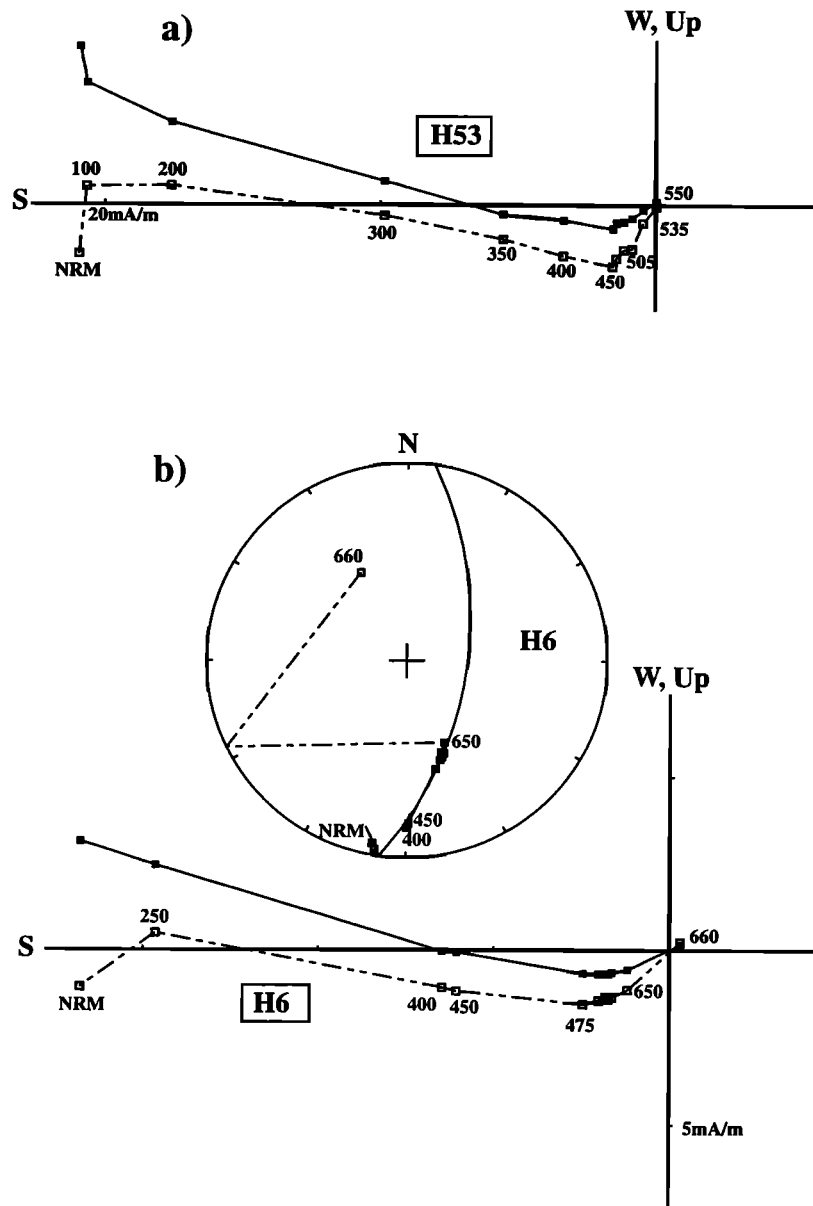


Figure 9. Examples of normal polarity high unblocking components from zones (a,c) N1 and (b) N2.

intervals, that is -1100 to -850 cm (covering N1 polarity zone) and -700 to -500 cm (covering N2 polarity zone), show no increase in the variance about the sample mean and thus do not exhibit a different degree or extent of diagenetic alteration when compared to horizons above and below.

Magnetostratigraphy and Reversal Asymmetry

Paleomagnetic data from this study, when combined with those of *Torsvik and Trench* [1991b] show the presence of five reverse and normal polarity intervals (R1→R5 and N1→N5) in the Ordovician Gullhøgen section (Figure 12). The lower section, that is, upper Arenig to lower Llandeilo, shows a relatively high reversal frequency, whereas the upper part of the section (Dalby Limestone: Middle Llandeilo–Caradoc) shows a relatively long time period of normal polarity. Due to the combined effects of low deposition rates (1–3 m/m.y.), that is, low time resolution, and the presence of local disconformities, most notable in the

Late Llanvirn and Early Llandeilo section (Figure 12), the observed reversal frequency can be considered as a minimum.

Normal polarity zones N3 to N5 (described as N1 to N3 by *Torsvik and Trench* [1991b]) are, to a first approximation, antipodal (see below and Table 1) to the reverse polarity zones (R1 to R5). It is apparent, however, that the late Arenig and early Llanvirn aged polarity zones N1–N2 differ by approximately 60° in declination from the other normal polarity directions and their reversed counterparts (Figures 8 and 13). It is noteworthy that the departures concern only declinations; the inclinations are equal within the α_{95} confidence limits. Normal polarity zones N1 and N2 do not share a common mean at the 95% confidence level [McFadden and Lowes, 1981] with the reversed polarity zones nor with other normal polarity zones. This prompts for an explanation in terms of (1) unresolved magnetization components with similar unblocking spectra, (2) postdepositional magnetic overprinting within strata containing the two anomalous normal polarity zones, (3) apparent polar

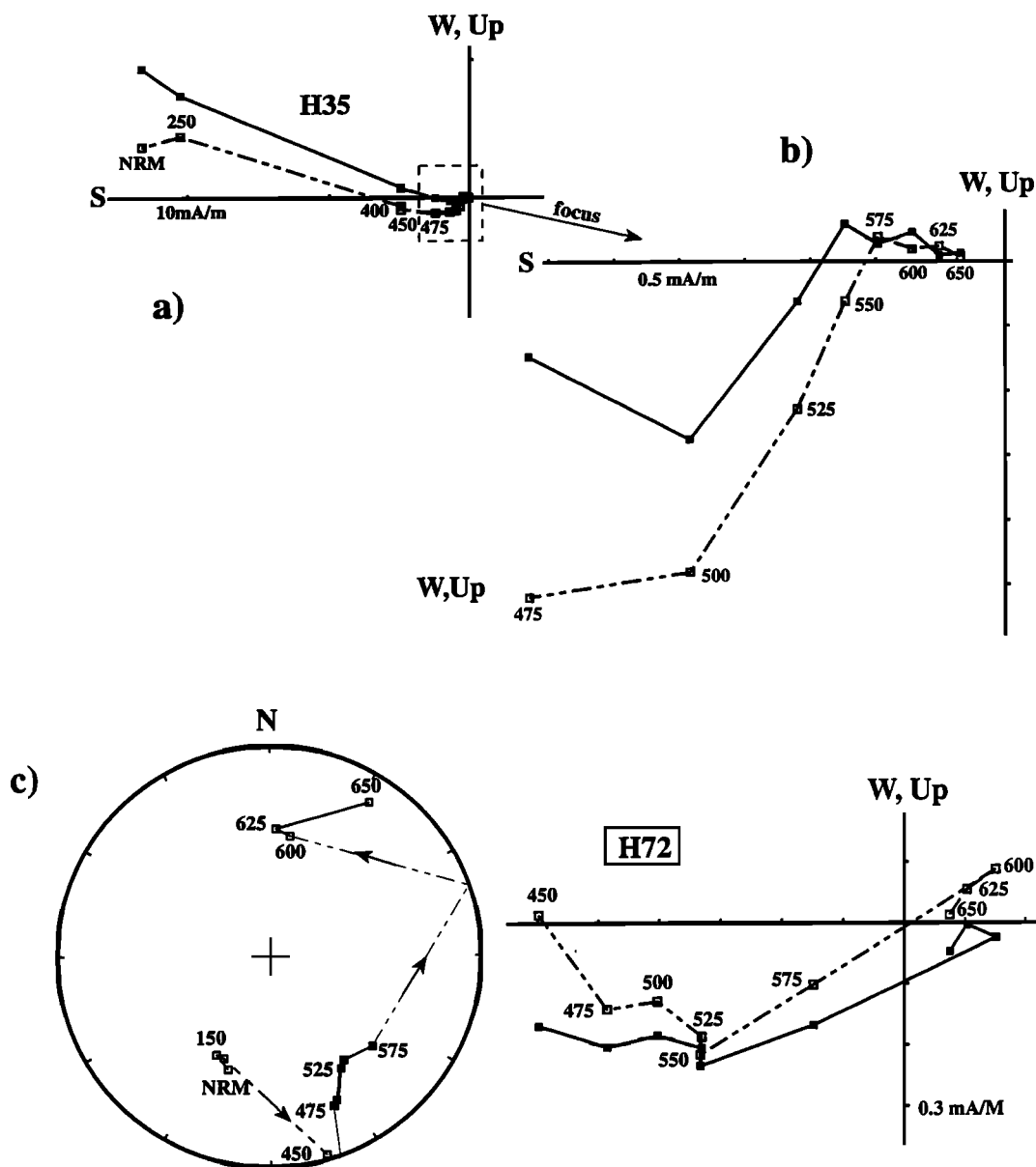


Figure 10. Examples of thermal demagnetization behavior. Reverse polarity zones (a) R2 and (b) R3.

wander (APW), or alternatively, (4) nondipole disturbances during this time interval.

Component Contamination

The distribution of polarity zone R3 directions indicates contamination of the P-C component (Figure 8e) which probably is caused by the fact that the P-C component occasionally may have similar or even higher unblocking temperatures than the primary Ordovician field direction (TCRM, secondary formed hematite). On the other hand, if the normal polarity zones N1 and N2 were systematically contaminated by the P-C component they should show a smeared directional distribution between the expected position of the antipodal direction for R1 and R2 (Figure 14) and the mean P-C component. They depict the opposite relationship, however, and their directional distribution then prompts for contamination of the reverse polarity directions. We note, however, that the distribution of normal polarity directions (Figure 14) do not fall on a greatcircle between the

reverse field directions and the expected normal paleofield; we therefore find this explanation unlikely.

Magnetic Overprinting

With the exception of R1 (gray limestone), all interval (R2 and R3 and N1-N2) have a hematite and magnetite host. The magnetomineralogy and the lithology appear similar, and we find it unlikely that the two normal polarity horizons were preferentially remagnetized at a younger time, for example by remagnetizing fluids. We do observe a peak in susceptibility across the N2 polarity transition, but the lack of shifts in either mean $\delta^{18}\text{O}$ or $\delta^{13}\text{C}$, or in their variation, across the normal polarity intervals (Figure 3) suggests that the normally and reversed magnetized lithologies have undergone comparable histories of diagenetic alteration so that the directional characteristics of the N1 and N2 polarity zones could not represent intervals of preferential alteration during post Ordovician times. We also note, if we consider this option, that

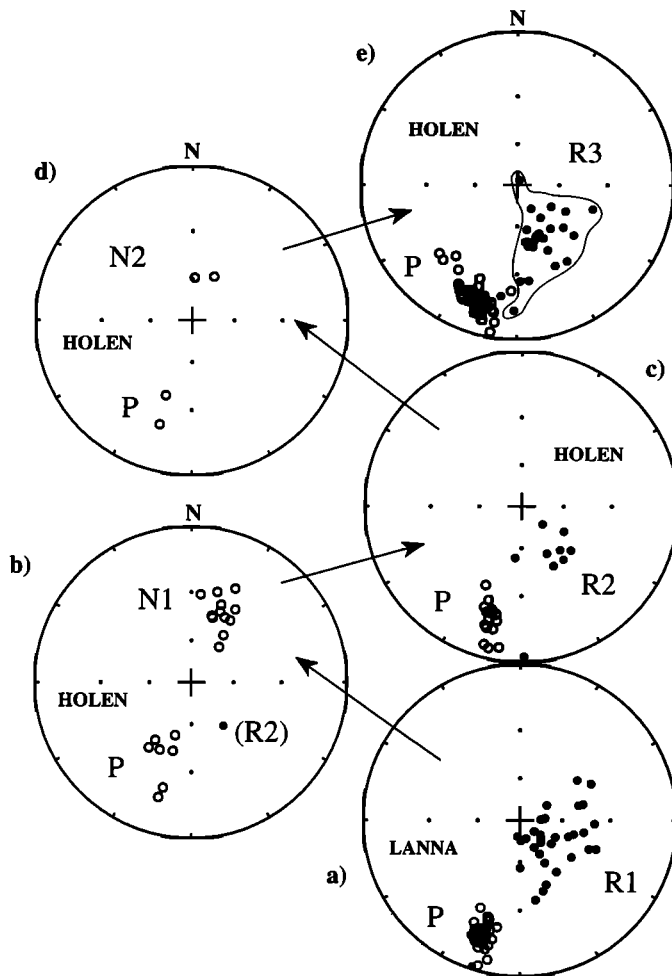


Figure 11. Examples of thermal demagnetization behavior for samples from polarity zone (a,b) R3 and the uppermost sampling level within (c) polarity zone N1.

the overprint direction does not fall on the post-Lower Ordovician APW path for Baltica [Torsvik et al., 1992].

Apparent Polar Wander

APW is ruled out since the observed reversal asymmetry has been identified at two successive normal polarity levels. If APW, it would require reversible, self-cancelling, APW to explain the reversal asymmetry. This is highly unlikely [e.g., Pesonen and Nevalinna, 1981].

Nondipole Field

Due to the lack of other reasonable explanations, we are inclined to believe that the normal polarity zones N1-N2 reflect a nondipole disturbance (million years scale) of the geomagnetic field in Late Arenig-Early Llanvirnian times (circa 476 Ma). Since the anomaly is mainly in declinations, the persistent nondipole field would be nonzonal, and such that it will preferentially bias declinations.

Paleopoles

The asymmetric normal polarity zones N1-N2 should not be used for apparent polar wander path construction. It is further evident that the elongated distribution of reverse polarity zone R3 (Figure 8), despite apparent linearity in Zijdeveld diagrams

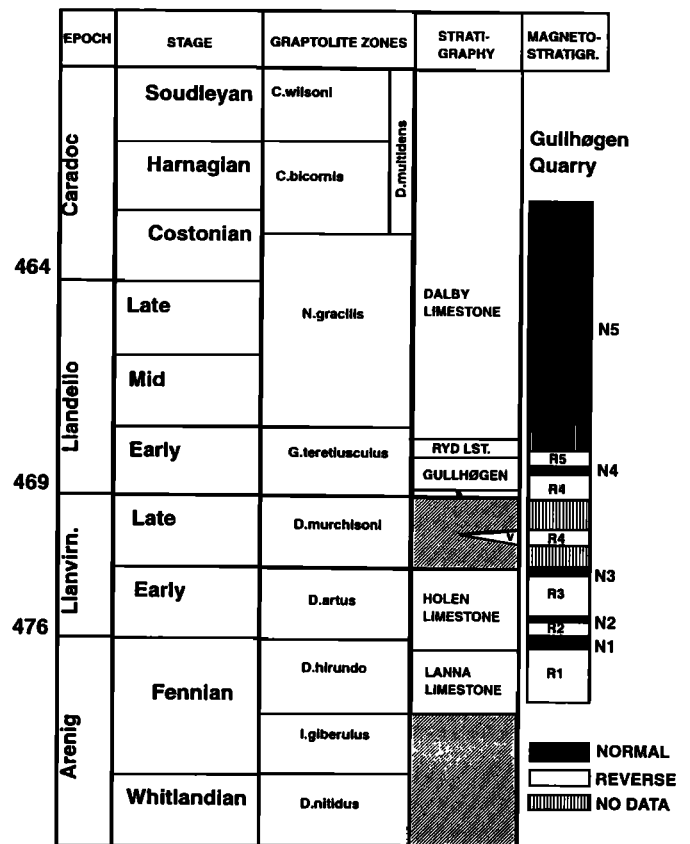


Figure 12. Magnetostratigraphy from the Gullhøgen Quarry section, local stratigraphy, graptolite zones and geological stage and epochs. Timescale after Harland et al [1989].

and low maximum angular deviations, suggest contamination by the P-C component. We consider that a combined mean of reverse polarity zones R1 and R2 provides the best estimate for the Late Arenig-Early Llanvirn (circa 476 Ma) paleofield. The combined mean pole (latitude=18.7°N, longitude=54°E; Table 1) compares well with Arenig-Llanvirn palaeopoles from other districts in Sweden (Table 2, Figure 15) and indicate that the

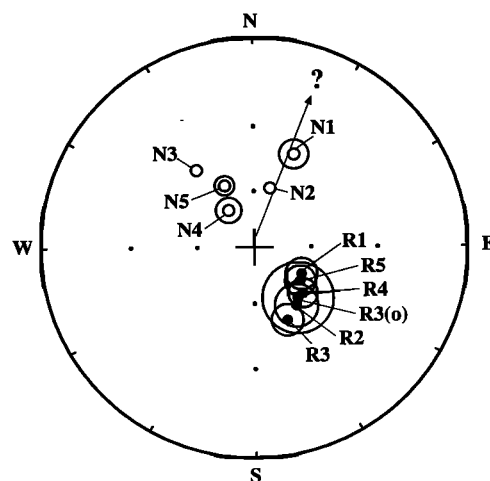


Figure 13. Mean directions obtained from polarity zones R1-R5 and N1-N4. R1-R3 and N1-N2 from the present study. R3(o)-R5 and N3-N5 after Torsvik and Trench [1991b]. (originally denoted R1-R3 and N1-N3 in their study).

Table 2. Ordovician Paleomagnetic Data From Scandinavia (Baltica)

Formation	α_{95}	P	Age	MA	Latitude	Longitude	References
Oslo Limestone	5.4	M	Late Ashgill	440	-5.3	6.5	1
Swedish Limestone I(N)	13.4	N	Late Llanvirn-Middle Caradoc	459	3.0	35.0	2
Gullhøgen (N5)	4.8	N	Middle-Llandeilo-Early Caradoc	465	5.0	34.0	3
Gullhøgen (N3,N4 and R3-5)	4.4	M	Early Llanvirn-Early Llandeilo	471	14.0	49.0	3
Gullhøgen (R1+R2)	6.8	R	Late Arenig/Early Llanvirn	476	18.7	54.0	4
Swedish Limestones	9.0	R	Arenig-Llanvirn	481	30.0	55.0	5
Swedish Limestones I(R)	5.1	R	Arenig-Llanvirn	481	18.0	46.0	2
Swedish limestones	2.2	R	Arenig-Llanvirn	481	30.0	46.0	6

Palaeomagnetic poles are plotted in Figure 15; P,= Polarity; N/R/M,= normal/reverse/mixed; Age,= epoch; E=Early; MA,= mean rock age in million years (timescale after *Harland et al.* [1989]; mean ages slightly modified after *Torsvik et al.* [1992]; Latitude/Longitude,= paleopole latitude /longitude; References are 1,= *Bøhm* [1989]; 2,= *Torsvik and Trench* [1991a]; 3,= *Torsvik and Trench* [1991b] (note that polarity zones were originally reported as R1-R3 and N1-N3); 4,= present study; 5,= *Claesson* [1978]; 6,= *Perroud et al.* [1992].

Farr et al. [1993] of sediments from North America. Their directional data, however, are extremely scattered, hence a detailed directional analysis leaves the issue unresolved. Conversely, the Siberian Lena River sections [e.g. *Rodionov*, 1966] contain a sedimentary break at this critical time interval [*Kanygin et al.*, 1988; *Trench et al.*, 1991, *Torsvik et al.*, 1995], hence it remains to be corroborated that the observed reversal asymmetry reflects a worldwide longlasting (million years scale) nondipole disturbance.

Acknowledgments. The Norwegian Research Council and NGU are thanked for financial support. Comments from Rob Van der Voo, H. Tanaka and L. J. Pesonen are appreciated.

References

- Bøhm, V., Vergleichende palaeomagnetische untersuchungen an verschiedenen Gesteinen des mitteleuropaischen Variszikums, Ph.D. thesis, 150 pp., Ludwig-Maximilians Univ., Munich, 1989.
- Claesson, K.C., Palaeomagnetic studies of Swedish Lower Palaeozoic rocks, Ph.D thesis, Univ. of Newcastle, Newcastle, New South Wales, 1977.
- Claesson, K.C., Swedish Ordovician limestones: Problems in clarifying their directions of magnetization, *Phys. Earth Planet. Inter.*, 16, 65-72, 1978.
- Craig, H., Isotopic standards for carbon and oxygen and correction factors for mass spectrometric analysis of carbon dioxide, *Geochim. Cosmochim. Acta*, 12, 133-140, 1957.
- Farr, M.R., D.R. Sprowl, and J. Johnson, Identification and initial correlation of magnetic reversals in the Lower to Middle Ordovician of Northern Arkansas, in *Applications of Palaeomagnetism to Sedimentary Geology*, vol. 99, edited by D.M. Aissaoui and N.F. Hurley, pp. 84-93, Society of Sedimentary Geology, Boulder, Colorado, 1993.
- Fisher, R.A., Dispersion on a sphere, *Proc. R. Soc. London A*, 217, 295-305, 1953.
- Harland, W.B., R.L. Armstrong, A.V. Cox, L.E. Craig, A.G. Smith, and D.G. Smith, *A Geological Time Scale*, Cambridge University Press, New York, 1989.
- Holmer, L.E., Lower Viruan discontinuity surfaces in central Sweden, *Geol. Foren. Stockholm Forh.*, 105, 29-42, 1983.
- Holmer, L.E., Middle Ordovician phosphatic inarticulate brachiopods from Västergötland and Dalarna, Sweden, *Fossils Strata*, 26, 1-172, 1989.
- Jaanusson, V., The Viruan (Middle Ordovician) of Kinnekulle and northern Billingen, *Bull. Geol. Inst. Univ. Uppsala*, 43, 1-73, 1964.
- Jaanusson, V., Ordovician of Västergötland, *Paleontol. Contrib. Univ. Oslo*, 279, 164-183, 1982.
- Kanygin, A.V., T.A. Moskalenko, and A.G. Yadrenkina, The Siberian Platform, in *The Ordovician System in Most of Russian Asia*, vol. 26, edited by R.J. Ross and J.A. Talent, pp. 1-27, International Union of Geological Sciences, Ottawa, Ontario, 1988.
- Lindström, M., Vom Anfang, Hochstand und Ende eines epikontinentalmeeres, *Geol. Rundsch.*, 60, 419-438, 1971.
- Lohmann, K.C., and J.G.C. Walker, The $\delta^{18}\text{O}$ record of Phanerozoic abiotic marine calcite cements, *Geophys. Res. Lett.*, 16, 319-322, 1989.
- McFadden, P.L., and F.J. Lowes, The discrimination of mean directions drawn from Fisher distributions, *Geophys. J. R. Astron. Soc.*, 67, 19-33, 1981.
- Mulder, F.G., Palaeomagnetic research in some parts of Central and Southern Sweden, *Sver. Geol. Unders. Ser. C*, 653, 1-64, 1971.
- Perroud, H., M. Robardet, and D.L. Bruton, Palaeomagnetic constraints upon the palaeogeographic position of the Baltic Shield in Ordovician, *Tectonophysics*, 201, 97-120, 1992.
- Pesonen, L.J., and H. Nevalinna, H., Late Precambrian Keweenawan asymmetric reversals, *Nature*, 294, 436-439, 1981.
- Rodionov, V.P., Dipole character of the Geomagnetic field in the Late Cambrian and the Ordovician in the south of the Siberian Platform, translated from Russian by E.R. Hope, pp. 94-101, Defense Research Board, Ottawa, Ont., 1966.
- Thorslund, P., Kambro-siluravlagringer utanfor fjall-kjedan, *Sver. Geol. Unders. Ser. B*, 16, 113-153, 1962.
- Thorslund, P., and V. Jaanusson, The Cambrian, Ordovician and Silurian in Västergötland, Närke, Dalarna and Jämtland, central Sweden, Guide to Excursions Nos. A23 and C18, pp. 1-51, in *International Geological Congress XXI Session*, Norden 1960, Lund, Sweden, 1960.
- Torsvik, T.H., and A. Trench, The Lower-Middle Ordovician of Scandinavia: Southern Sweden 'revisited', *Phys. Earth Planet. Inter.*, 65, 283-291, 1991a.
- Torsvik, T.H., and A. Trench, Ordovician magnetostratigraphy: Llanvirn-Caradoc limestones of the Baltic Platform, *Geophys. J. Int.*, 107, 171-184, 1991b.
- Torsvik, T.H., M.A. Smethurst, R. Van der Voo, A. Trench, N. Abrahamsen, and E. Halvorsen, BALTICA - A synopsis of Vendian-Permian palaeomagnetic data and their palaeotectonic implications, *Earth Sci. Rev.*, 33, 133-152, 1992.
- Torsvik, T.H., J. Tait, V. Moralev, W.S. McKerrow, B.A. Sturt, B.A., and D. Roberts, Ordovician Palaeogeography of Siberia and adjacent plates, *J. Geol. Soc. London*, 152, 279-287.
- Trench, A., W.S. McKerrow, and T.H. Torsvik, Ordovician Magnetostratigraphy: A correlation of global data, *J. Geol. Soc. London*, 148, 949-957, 1991.

Veizer, J., W.T. Holsen, and C.K. Wilgus, Correlation of $^{13}\text{C}/^{12}\text{C}$ and $^{34}\text{S}/^{32}\text{S}$ secular variations, *Geochim. Cosmochim. Acta*, 44, 579-588, 1980.

S. Dunn and K.C. Lohmann, Department of Geological Sciences, University of Michigan, 1006 C.C. Little Building, Ann Arbor, MI 48109.

T.H. Torsvik, Geological Survey of Norway, P.B. 3006 Lade, N-7002 Trondheim, Norway. (fax: 47-73-904494; e-mail: trond.torsvik@ngu.no)

A. Trench, Western Mining Corporation, Kambaldi Nickel Mines, P.O. Kambalda, W.A. 6442, Western Australia, Australia.

(Received October 6, 1994; revised February 6, 1995; accepted February 23, 1995.)